

ON THE STRENGTHENING OF ALUMINIUM ALLOY 6056T6

Marie VIVAS*, Philippe LOURS*, Christophe LEVAILLANT*,
Marie-José CASANOVE**, Alain COURET** and Armand COUJOU**

* Centre Matériaux, Ecole des Mines d'Albi-Carmaux,
Campus Jarlard, 81013 Albi cedex 09, France.

** CEMES-LOE, 29 rue Jeanne Marvig,
BP 4347, 31055 Toulouse cedex, France.

ABSTRACT Conventional and *in situ* straining Transmission Electron Microscopies are used to characterize the precipitates and the deformation mechanisms in aluminium alloy 6056T6. It is shown that, depending on the size of precipitates, either precipitate shearing or by-passing with formation of loops occurs as dislocations propagate in the alloy. Shearing, or more precisely the resistance of precipitates to shearing, is the predominant hardening mechanism in aluminium alloy 6056 T6. The maximum force an individual precipitate can sustain before being sheared by dislocations is calculated which leads to a satisfactory estimation of the flow stress of the alloy.

Keywords : *Transmission Electron Microscopy, in situ straining TEM, dislocation, precipitate, shearing, aluminium alloy 6056T6*

1. INTRODUCTION

Because of its good mechanical properties as well as improved corrosion resistance and weldability, aluminium alloy 6056 is being investigated as it may substitute for standard 2024 alloy for the manufacturing of aircraft fuselage skins. The high flow stress of the alloy, decreasing from 355 MPa at room temperature to 315 MPa at 125°C [1], is due to appropriate thermal treatment which provides the precipitation of finely distributed second phase particles with which dislocations interact while the alloy is strained.

Strengthening models include parameters such as the volume fraction of precipitates, the mean distance of precipitates along dislocation lines under load and the maximum strength precipitates can sustain before being sheared by dislocations [2, 3, 4]. The size distribution of precipitates is also important because the smallest precipitates, easily sheared by dislocations, and the few largest precipitates, by-passed by dislocations, do not contribute effectively to hardening.

The aim of the study is to correlate the mechanical properties to the microstructure of the alloy and its evolution under load using Transmission Electron Microscopy (TEM). In order to address the level of flow stress shown by the alloy, particular focus is placed on the quantitative determination of the morphology and size of precipitates which interact effectively with dislocations as well as on the strength that individual precipitates oppose to dislocation glide.

2. EXPERIMENTAL DETAILS

Table 1 gives the chemical composition of aluminium alloy 6056T6 kindly provided by Péchiney CRV. The alloy is solution heat treated at 550°C, water quenched and tempered at 175°C during 8 h.

Al	Si	Mg	Cu	Mn	Fe	Zn	Zr	Cr	Ti
balance	0.943	0.869	0.798	0.634	0.198	0.153	0.11	0.066	0.039

Table 1 : Chemical composition of alloy 6056 (weight %).

High Resolution Transmission Electron Microscopy (HRTEM), conventional TEM and *in situ* straining TEM are utilized to investigate both the microstructure of the free-stress alloy and the deformation mechanisms at the scale of the dislocation/precipitate interaction.

3. MICROSTRUCTURE OF THE ALLOY

Fig. 1 is a dark-field image, taken with the precipitate reflections around a forbidden 110 matrix spot, showing the microstructure of the alloy as-treated prior to any straining. Large dispersoids D_1 and D_2 , mainly localized on the grain boundaries (J_1, J_2), can be seen on the figure; these do not play a prevalent role in the strengthening. A precipitate free zone (PFZ) about 50 nm wide is also visible.

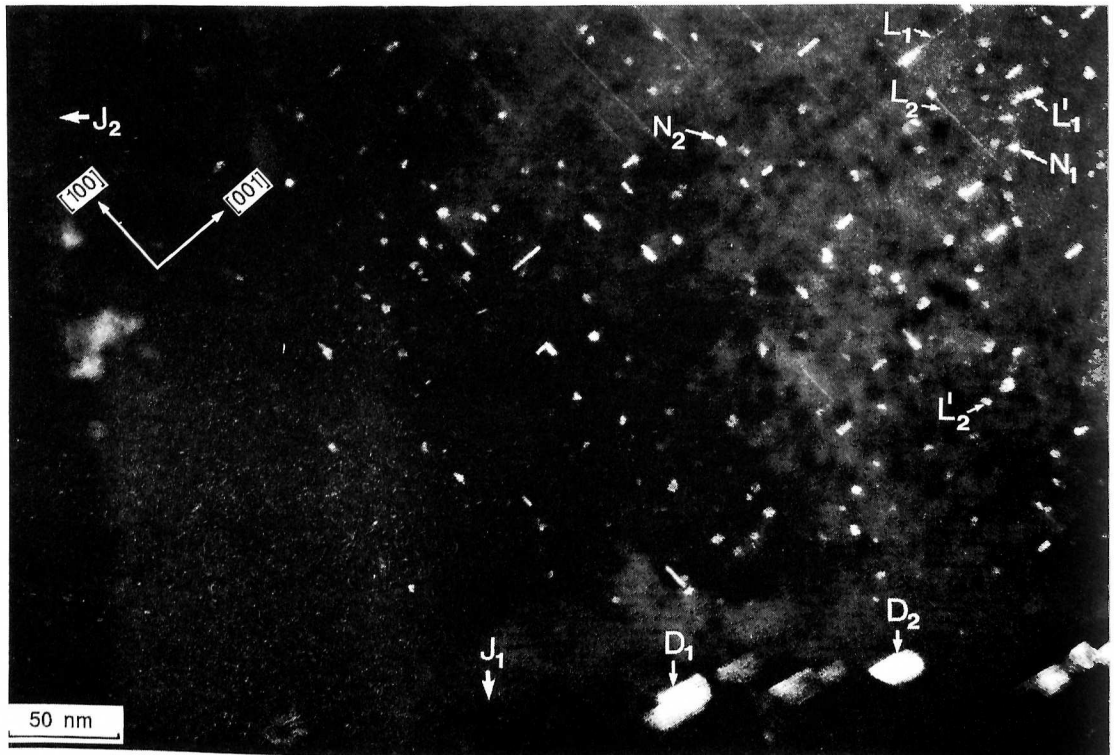


Figure 1 : General TEM micrograph of the alloy microstructure.

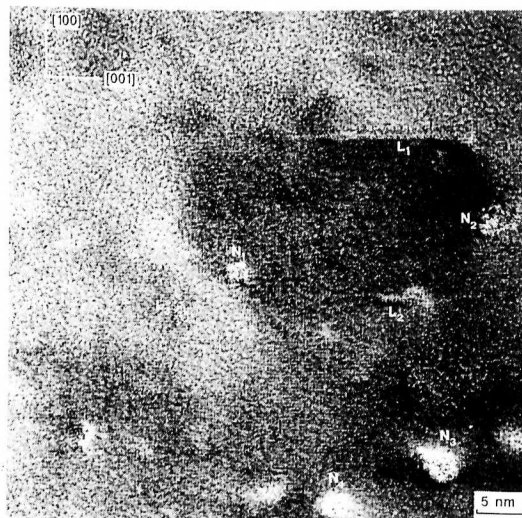


Figure 2 : $[010]$ zone axis bright field image of the alloy microstructure.

On Fig. 1, the precipitates shown are either laths viewed with their longitudinal cross-section parallel to the foil (L_1, L_2) or needles viewed edge-on (N_1, N_2). Most precipitates lie along the three $\langle 100 \rangle$ directions of the aluminium matrix showing a homogeneous and isotropic distribution [4, 5]. Note that only few precipitates with rectangular cross-sections, marked L'_1 and L'_2 , deviate from $\langle 100 \rangle$ by about 10° . The imaging of precipitates on a TEM micrograph is directly related to the precipitate thickness crossed by the electron beam. As a consequence, only the largest precipitates with cross-section parallel to the foil can be imaged and a thorough examination of Fig. 1 shows that only about one precipitate viewed side-on in twenty is visible. The mean length of visible precipitates is measured to be about 66 nm [5]. The volume densities of laths ($N_L/V = 1.3 \cdot 10^{16} \text{ cm}^{-3}$) and needles ($N_N/V = 10^{17} \text{ cm}^{-3}$) are calculated by counting those precipitates edge-on, then multiplying by three to get the total number of precipitates and finally dividing by the volume of material investigated. The total volume density of precipitates ($N/V = N_L/V + N_N/V$) is about $1.13 \cdot 10^{17} \text{ cm}^{-3}$ in good agreement with previous results [6]. Fig. 2 is a higher magnification micrograph showing edge-on needles (N_1, N_2, N_3, N_4) and laths with either longitudinal (L_1) or transverse cross-sections (L_2, L_3) parallel to the foil. From that type of images, the distribution of cross-sections of both laths and needles is evaluated. These range from 3 to 12 nm^2 (mean value 6.5 nm^2) for laths and from 2.6 to 16 nm^2 (mean value 7 nm^2) for needles as shown on the histogram of Fig. 3.

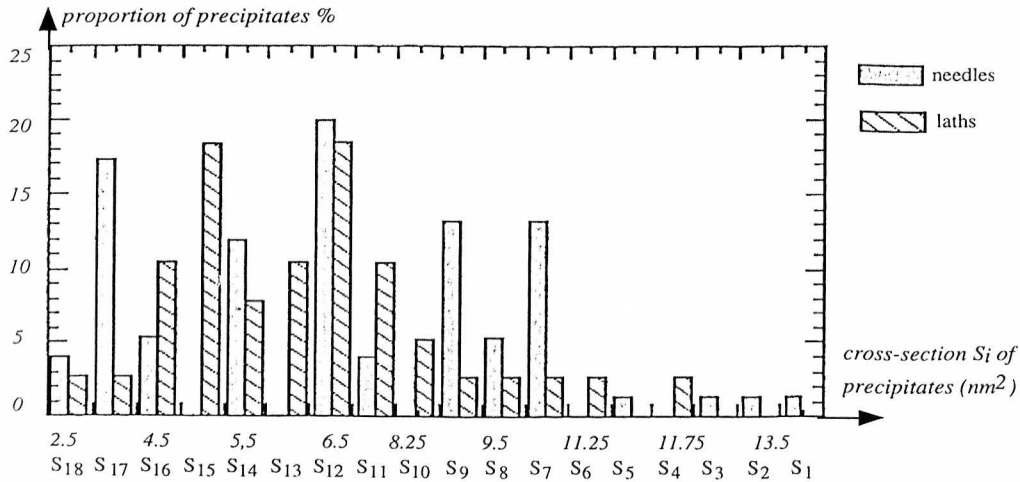


Figure 3 : Histogram of the proportion of precipitates versus the cross-section areas.

4. SHEARING OF PRECIPITATES

4.1 Mean distance between precipitates that pin dislocations

Under load, some precipitates are able to pin dislocations before being sheared and before dislocations advance to new obstacles. From appropriate frames of a video tape recording of TEM *in situ* straining experiments such as Fig. 4, the distances between those precipitates interacting with dislocations are derived. According to our measurements, this distance shows a nearly Gaussian distribution ranging from 5 to 81 nm with an average value of about 30 nm.

4.2 Volume fraction of precipitates contributing to strengthening

The volume density of precipitates which effectively interact with dislocations (N'/V) can be calculated from the mean distance between precipitates along the dislocation lines. Assuming a homogeneous square distribution of precipitates, a trivial calculation shows that the volume density of those precipitates can be expressed by $N'/V = \sqrt{3}/2hd^2 = 1.46 \cdot 10^{16} \text{ cm}^{-3}$ where h is the mean length of precipitates (66 nm) and d the mean distance between precipitates.

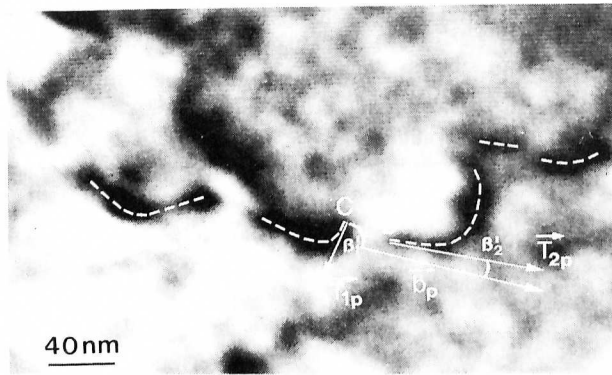


Figure 4 : Frame from a video tape recording of an *in situ* straining experiment at room temperature showing a dislocation in critical position prior to shear precipitates.

From the value N/V and the data of the histogram of Fig. 3, the minimum critical cross-section of precipitates that control the deformation of the alloy as well as the proportion of those precipitates can be determined. The calculation consists in determining the integer j and the associated cross-section S_j for which :

$$\sum_{i=1}^{i=j} \left[P_i^L \left(\frac{N_L}{V} \right) + P_i^N \left(\frac{N_N}{V} \right) \right] = N/V \quad (1)$$

where P_i^L and P_i^N are the proportions of laths and needles respectively, with cross-section S_i .

The calculation yields to a critical area $S_j = 10.5 \text{ nm}^2$ and a proportion of laths and needles respectively of 8% and 19%. Taking a mean value of the cross-sections greater than S_j of 12.5 nm^2 , the volume fraction of efficient precipitates is about 1.2 % which represents, according to results by [6], about half of the total volume fraction of precipitates.

4.3. Maximum strength of precipitates and estimation of the flow stress

From *in situ* micrographs such as in Fig. 4, the maximum strength sustained by precipitates before being sheared by dislocations can be derived [4]. This is performed in the frame of the orientation-dependent line tension model using geometric parameters $\beta_1 = 72^\circ$ and $\beta_2 = 26^\circ$ and line tensions $T_1 = 0.21 \text{ nN}$ and $T_2 = 0.61 \text{ nN}$. The angles and line tensions projected in the dislocation slip plane are shown on Fig. 4. The calculation leads to a maximum strength F_m of about 0.78 nN (the mean value of F_m for twenty various cases is 0.6 nN). This allows us to estimate the critical resolved shear stress $\tau = F_m / d \cdot b = 130 \text{ MPa}$ necessary to propagate a dislocation with Burgers vector b in a distribution of precipitates separated by an average distance d . From this and according to Taylor's theory, one finds a satisfactory value of the flow stress for the polycrystal of 390 MPa.

5. BY-PASSING OF PRECIPITATES

As discussed above, precipitates with cross-sections smaller than S_j do not contribute effectively to strengthening as they are assumed to be easily sheared by dislocations when the alloy is strained. On the other hand, very large precipitates are by-passed by dislocations and they too do not contribute so much to hardening since they are present in small quantities. Fig. 5 is a video tape recording of an *in situ* straining experiment performed at room temperature under bright field conditions. Fig. 5 (a) corresponds to the initial stage of deformation. From Fig. 5 (a) to Fig. 5 (b), a dislocation d enters the investigated zone and stops on precipitates in A, B, C, D, E, F, G and H. From Fig. 5 (b) to Fig. 5 (c), the dislocation escapes from all obstacles and leaves loops behind it (for instance in B or E). It is

assumed that precipitates located in *B* and *E* are too large to be sheared and that a preferential by-passing mechanism occurs. Due to the compensatory effect of associated strain fields, dislocations and precipitates cannot be adequately imaged simultaneously, which prevents the measurement of the critical cross-section of precipitates that are by-passed by dislocations.

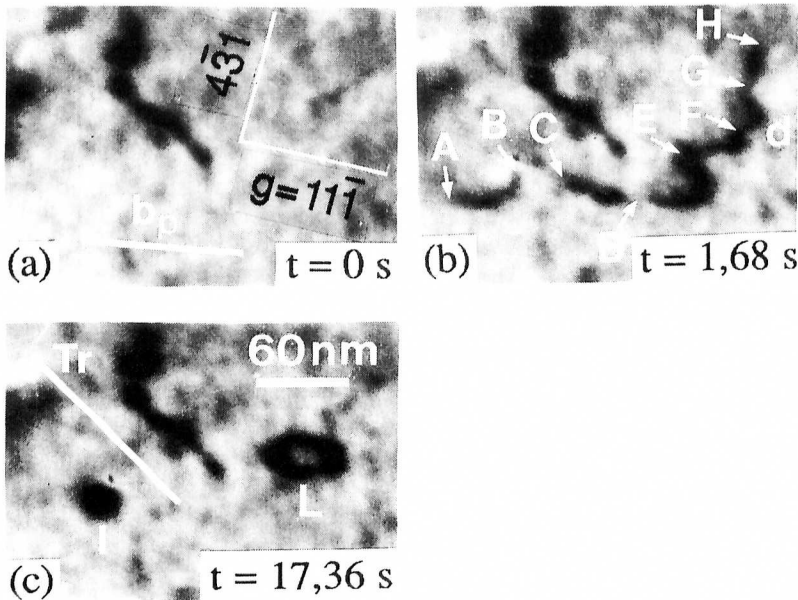


Figure 5 : In situ straining sequence at room temperature showing the by-passing of precipitates assisted by the formation of dislocation loops.

As the loops formed are able to spread under subsequent loading [5], it is concluded that they are not Orowan loops but three dimensional loops created by the double cross-slip of adjacent dislocation segments according to Fig. 6. As cross-slip may be thermally activated, enhanced by-passing occurs at high temperature, while at low temperature (-110°C), some Orowan loops form [5].

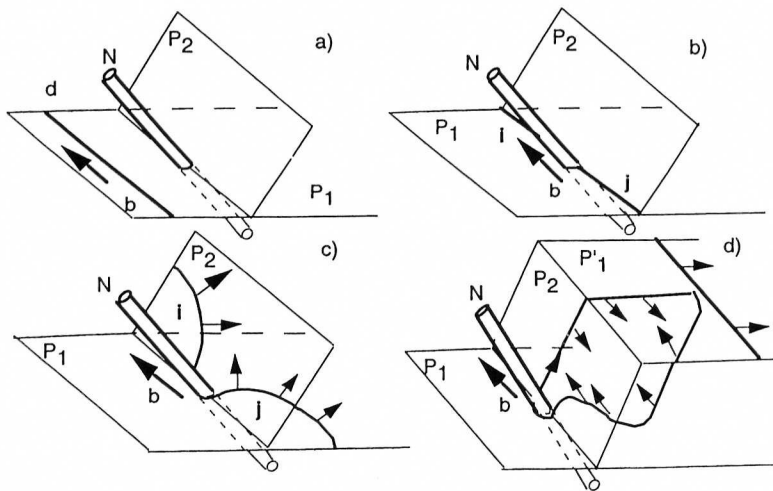


Figure 6 : Mechanism of formation of a three dimensional loop as dislocation by-passes a precipitate.

6. CONCLUSION

The morphology and size of the various precipitates present in aluminium alloy 6056T6 have been identified using Transmission Electron Microscopy. *In situ* straining experiments performed at room temperature show that dislocation propagation in the material can proceed either by precipitate shearing or precipitate by-passing.

Precipitates with a cross-section smaller than a critical value S_j do not contribute effectively to the hardening as they are easily sheared by moving dislocations. Precipitates with a cross-section greater than S_j , which represents about half of the total volume fraction of precipitates, are able to pin dislocations and greatly harden the material. This is the prevalent strengthening mechanism in the material and the maximum strength precipitates can sustain before being sheared by dislocations has been calculated which yields a rather good estimate of the alloy flow stress.

However, beyond a certain value of the cross-section, precipitate shearing no longer occurs and particles are by-passed by dislocations with concomitant formation and spreading of three dimensional loops. This formation is nevertheless rather rare as only few precipitates shows high enough cross-section to be preferentially by-passed. Though this contributes to the multiplication of dislocations which may induce strain-hardening, it is not regarded as a major strengthening mechanism.

REFERENCES

- [1] M. Vivas, P. Lours, C. Levailant, A. Couret, M.-J. Casanove, A. Coujou : in Proceedings of the Fifth International Conference on Aluminium Alloys (Part 2), Eds. J.-H. Driver, B. Dubost, F. Durand, R. Fougères, P. Guyot, P. Sainfort, M. Suery, Grenoble, France, (1996), 1305.
- [2] L. M. Brown, R. K. Ham : in Strengthening Methods in Crystals, Eds. A. Kelly, R. B. Nicholson, (1971), 9.
- [3] V. Gerold : in Dislocations in Solids, F. R. N. Nabarro, (1979), 221.
- [4] M. Vivas, P. Lours, C. Levailant, A. Couret, M.-J. Casanove, A. Coujou : Phil. Mag. A, 76 (1997), 921.
- [5] M. Vivas : Thèse de Doctorat de l'Université Paul Sabatier, Toulouse, (1997).
- [6] P. Donnadiou, F. Carsughi, A. Redjamia, C. Diot, G. Lapasset : J. of Applied Crystallography, (in press).